

available at www.sciencedirect.comjournal homepage: www.elsevier.com/locate/compag

Mapping irrigated area in Mediterranean basins using low cost satellite Earth Observation

Thomas K. Alexandridis^{a,b,*}, George C. Zalidis^b, Nikolaos G. Silleos^a

^a Laboratory of Remote Sensing and GIS, School of Agriculture, Aristotle University of Thessaloniki, Thessaloniki 54124, Greece

^b Laboratory of Applied Soil Science, School of Agriculture, Aristotle University of Thessaloniki, Thessaloniki 54124, Greece

ARTICLE INFO

Article history:

Received 19 January 2008

Received in revised form

15 April 2008

Accepted 15 April 2008

Keywords:

Satellite remote sensing

Image enhancement

Feature mapping

Irrigated area

ABSTRACT

Excessive use of irrigated water in the Mediterranean has deteriorated the freshwater resources by depleting the aquifers, discharging agri-chemicals and accelerating saltwater intrusion. Several European directives outline that estimating the extent of irrigated areas in each water basin is a primary step towards sustainable natural resources management. This paper aims to identify a low cost methodology for mapping irrigated area in Mediterranean basins, using satellite Earth Observation. After evaluating several combinations of land feature mapping techniques on digitally enhanced satellite images, the one with the highest accuracy has been identified (thresholding of the second principal component). The methodology was formulated under the assumption that irrigated land can be identified by the result of irrigation, i.e. the existence of green vegetation in the semiarid summer, thus avoiding costly field surveys, and using low cost satellite imagery. The proposed methodology has been applied to two Mediterranean basins with conflicting agronomic and ecological interests, which were of a different scale. The resulting irrigated area map achieved high accuracy (up to 98.4%) and reliability (k up to 0.967) in both basins. The results were also displayed as irrigation intensity to improve visualisation and help identify areas of high environmental pressure on nearby wetlands.

© 2008 Elsevier B.V. All rights reserved.

1. Introduction

Irrigation is crucial to meet food demand, as it increases yields of most crops by 100–400%. Over the past 30 years, the global irrigated area expanded by about 1.6% a year, resulting in a total increase of 1,000,000 km² during 1962–1998. Thus, global freshwater consumption rose sixfold between 1900 and 1995—more than twice the rate of population growth (FAO and IFAD, 2006). With irrigation being the primary freshwater consumer (Seckler et al., 1999; Shiklomanov, 2000), it is essential to have an up-to-date estimate of irrigated area extents, if we hope to achieve sustainable management of water resources.

Monitoring irrigated crops on a national scale provides a good estimate of the expected production, allowing policies and strategies to be formulated and avoid food or environmental crises (Bastiaanssen et al., 2000). Furthermore, mapping the annual extents of irrigated fields at the local level assists the collection of water fees and supports equity in water rights (Bastiaanssen, 1999). Several hydrological models have been developed to estimate water requirements and water use for irrigation (Babajimopoulos et al., 1995; Droogers et al., 2000; Kite, 2000), however they still depend on an external estimate of the spatial distribution of irrigated land to operate on.

* Corresponding author at: Laboratory of Remote Sensing and GIS, School of Agriculture, Aristotle University of Thessaloniki, University Box 259, Thessaloniki 54124, Greece. Tel.: +302310 991778; fax: +302310 991778.

E-mail address: thalex@agro.auth.gr (T.K. Alexandridis).

0168-1699/\$ – see front matter © 2008 Elsevier B.V. All rights reserved.

doi:10.1016/j.compag.2008.04.001

Statistics from an agricultural census can be biased towards higher values when they are collected for subsidised crops, or towards lower values when water fees are area-based (Droogers, 2002; Biggs et al., 2006). Moreover, information from ground sources is often based on irrigation system design data rather than actual measured figures (Bastiaanssen et al., 2000). Remote sensing has been extensively used in the last three decades, as it provides objective measurements of wide coverage at high resolution and specialised wavelengths. Early studies used visual interpretation (Heller and Johnson, 1979; Nageswara Rao and Rao, 1987) of printed colour composites from Landsat images. Several digital image processing algorithms have been tested for mapping irrigated areas, such as supervised classification of original image bands (Thiruvengadachari, 1981), vegetation indices (Xiao et al., 2002), multi-stage classification (El-Magd and Tanton, 2003), and other more sophisticated methods such as classification of image time series (Thenkabail et al., 2005; Biggs et al., 2006) and fuzzy neural networks optimised with structure learning and genetic algorithms (Mitrakis et al., 2008). Most of these studies utilise the spectral characteristics of chlorophyll in the red and near-infrared wavelengths, while others use shortwave-infrared (Nageswara Rao and Mohankumar, 1994; Thenkabail et al., 2005), and thermal infrared (Vidal and Perrier, 1990). These methods have been applied at various scales, from the field level (Lourens, 1990; El-Magd and Tanton, 2003) to large river basins (Thenkabail et al., 2005; Biggs et al., 2006), demonstrating their wide range of applicability.

In Europe, mainly in the Mediterranean, excessive use of irrigated water has deteriorated the freshwater resources by depleting the aquifers, discharging agri-chemicals and accelerating saltwater intrusion. To alleviate these threats, the European Commission (EC, 2000) has initiated the Water Framework Directive (WFD), with the general objectives of improving water quality, guaranteeing provision of sufficient quantities of good quality water for all purposes, and avoiding any long-term deterioration. Among others, the WFD demands the identification of pressures from agriculture and estimation of water abstractions, with the overall aim to recover the costs of water services, including environmental and resource costs. A crucial step in this direction is the knowledge of the area and location of the irrigated agriculture. Following this trend, the recent reform of the Common Agricultural Policy (CAP) of the EU (EC, 2003) has shifted the focus from subsidising irrigated crops towards sustainable agriculture to promote environmental safeguards and ensure future yields. In this context, the legal framework for monitoring and control of irrigated area in the EU has been set for various purposes: from subsidies to set-aside (EC, 1999a; EC, 1999b). The WFD dictates that monitoring should be performed at the basin level. Although scale specifications are not defined, detailed mapping is required in the fragmented Mediterranean agricultural environment, thereby increasing the cost of monitoring (Lianos and Parliariou, 1986).

Thus, the continuously changing character of agricultural crop pattern at various spatial and temporal scales in response to management decisions, agricultural policies, prices, irrigation water availability and environmental factors, among others, makes remote sensing technology a necessary tool

for application in this field (Martinez-Casasnovas et al., 2005). Considering the above, there is a need for a methodology that can be implemented during the monitoring and control procedures dictated by the European directives, policies and regulations, bearing the following features: low cost input data (satellite images and fieldwork), low cost methods (standard software and low implementation of highly trained personnel), high accuracy, and objectively repeatable (based on solid assumptions). The aim of this work is to develop a methodology that satisfies these needs, and test it in two Greek basins to demonstrate its applicability at various scales.

2. Materials and methods

2.1. Study areas

2.1.1. Test site: Mygdonia basin

The test site is the Mygdonia basin, which is located in a tectonic depression in northern Greece (Fig. 1). Its watershed covers an area of 2100 km², and includes lakes Koronia and Volvi, which form an extended wetland. The climate of the region is Mediterranean, and annual rainfall ranges from 400 to 450 mm, distributed almost entirely during the winter season, and without any significant precipitation during the summer season. The surface flow through streams is seasonal and intermittent, however, a continuous subsurface discharge feeds the lakes throughout the year. The alluvial plane on the lower part of the basin favoured the development of a shallow (around 40 m depth) and a deeper under pressure aquifer (lower than 150 m) (Zalidis et al., 2004).

The wetland ecosystem is surrounded by an intensively cultivated agricultural area. The dominant agricultural crops are maize, alfalfa, and cereals. Cereals are rain-fed winter crops, sown in early December and harvested in late May. Maize and alfalfa are the irrigated summer crops, sown in April and harvested at the end of the irrigation season (late September to early October). Maize and alfalfa production are essential parts of the local economy, supporting the numerous livestock farms that are spread around the slopes of the basin. There is no exploitation of surface water, and the only source of fresh water for irrigation is through groundwater resources. Numerous privately owned pump wells, often illegal, were installed in the 1980s, which are exploiting the shallow groundwater aquifer. Since then, water abstraction has increased drastically because of the expansion of the irrigated area and the use of low application efficiency irrigation systems.

Irrigated agriculture is an important economic activity in the area, but recent development has resulted in the depletion of the shallow aquifer, and a subsequent decrease in the lakes' water level. Lake Koronia in particular, which is shallow (max depth 5 m before 1980) and has the highest concentrates most of the irrigated fields, had its water level decreased by 80% (Alexandridis et al., 2007) since 1980. As a result, the natural ecosystem has suffered severe degradation, with a significant loss of volume and habitat heterogeneity. In recognition of its ecological importance, and to prevent further degradation, the wetland system of lakes Koronia and Volvi is protected by several legal and binding actions: it is a Wetland of International

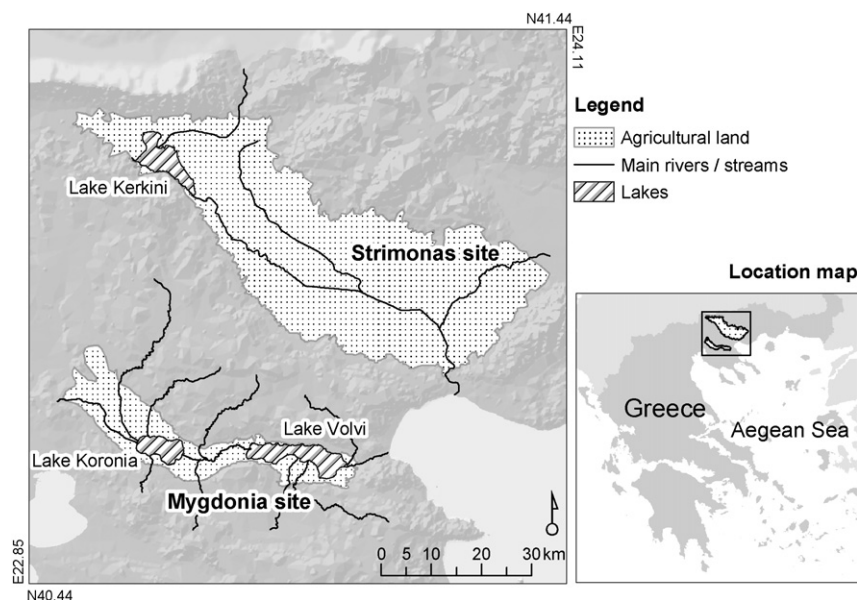


Fig. 1 – Location map and main characteristics of the study areas: Mygdonia and Strimonas site.

Importance according to Ramsar Convention (site code 57, area 163.88 km²), a Special Protected Area designated by the implementation of European Birds Directive (EEC, 1979) (site code GR1220009, area 156.71 km²), and a Site of Community Importance following the implementation of European Habitat Directive (EEC, 1992) (site code GR1220001, area 269.47 km²).

2.1.2. Demonstration site: Strimonas basin

The demonstration site is the Greek part of the Strimonas river basin (Fig. 1). The total basin of the trans-boundary river covers an area of 17,250 km², with its upstream areas situated in Bulgaria (65% of total area). A large reservoir (artificial lake Kerkini) was constructed in the 1930s immediately upstream of the Strimonas plain in Greece, to store water for irrigation and to prevent flood events. With progressive drainage works, agricultural land has been reclaimed from the wetlands and temporary lakes that had been dominating the floodplain of Strimonas. By the 1960s, an extended irrigation system had been developed in the plain (the largest in Greece), which taps water from the reservoir and river diversion dams. Water is distributed mainly by open canals, which are predominantly lined but often badly maintained, thus with low conveyance efficiencies. Local groundwater pumping stations provide supplementary water to account for the inefficient operation of the irrigation system. The large quantities of drainage water are reused for irrigating downstream regions. The total irrigated area is estimated to exceed 800 km², including the areas irrigated by privately operated pump wells (upper reaches). The main agricultural crops are irrigated maize, cotton, rice, beetroot, alfalfa, and rain-fed winter cereals. Agricultural and livestock production are the main economic activities in the site.

Artificial lake Kerkini has been recognised as a wetland of international importance (Ramsar site code 58, area 109.9 km²). It is also part of a Special Protected Area (site code GR1260008, area 277.1 km²) and a Site of Community Impor-

tance (site code GR1260001, area 783.2 km²). Due to the lake's operation as an irrigation reservoir, its water level fluctuates by 5 m during the irrigation season (May–September) and its surface decreases from 75 km² in spring to 50 km² in early autumn. As a result, the riparian forest and other key wetland habitats have decreased drastically. It is a case of upstream ecosystems receiving the impact of downstream agricultural activities. Another Site of Community Importance (site code GR1260002, area 12.9 km²) is the Strimonas estuary, which suffers from low water quality due to agricultural drainage and low discharge during the irrigation season, which is not sufficient to sustain the coastal ecosystem.

2.2. Datasets

2.2.1. Satellite images

A satellite image acquired on July 16, 2003 by the ASTER (Advanced Spaceborne Thermal Emission and Reflection Radiometer) sensor on board the Terra satellite (launched in December 1999) was used. It covers the entire Mygdonia basin with a spatial resolution (ground distance sampling) of 15 m in visible and near-infrared wavelengths, and 30 m in shortwave-infrared. A SPOT-4 HRV (Système Pour l'Observation de la Terre 4 – Haute Resolution Visible, launched in March 1998) satellite image was also utilised, acquired during the same cropping season, on September 23, 2003. The SPOT image covers the western side of the site only, where most of the irrigated area is located. The two satellite images are displayed in Fig. 2 in standard false colour composite (R, G, B = green, red, near-infrared), where green photosynthesising vegetation (natural and cultivated) appears in vivid red colour, and harvested wheat fields and grassland appear in pale green. Lakes Koronia (west) and Volvi (east) appear in dark blue and black, respectively. Comparing the two images, less irrigated fields are evident in September, due to the harvesting of early maize.

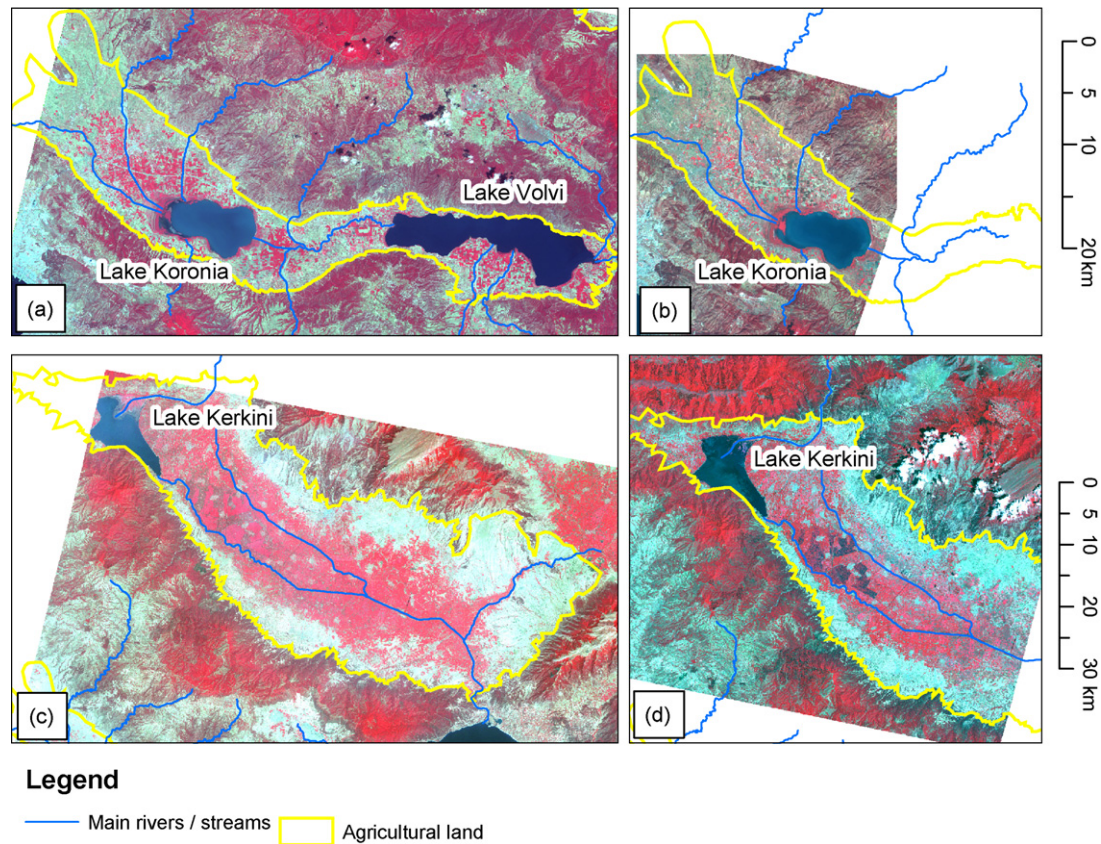


Fig. 2 – Satellite images used in Mygdonia site: ASTER/Terra (a), SPOT-4 HRV (b), and in Strimonas site: Landsat 7 ETM+ (c and d).

Two Landsat 7 ETM+ (Enhanced Thematic Mapper+, launched in April 1999, substituted by Landsat 5 TM after a malfunction in 2003) images were used for Strimonas site. Both were acquired during the same cropping season (June 24 and August 24, 2000), and cover the site with a spatial resolution of 30 m in visible, near-infrared and shortwave-infrared. A lower spatial resolution was accepted in this site, as the geographic scale (extents of the study area) is nearly 10 times larger than the Mygdonia site. The two satellite images are displayed in Fig. 2 in standard false colour composite. Lake Kerkini appears in dark blue in the north. Comparing the two images, more irrigated fields appear in August, as summer crops are in full development.

2.2.2. Sampling points for training and validation

Sampling areas for algorithm training and results validation are normally collected by the use of field surveys in the same cropping season as the satellite image acquisition. This often constitutes the largest cost of the mapping project, depending on the sampling design and accessibility of the sample locations. However, when the mapped features are evidently identified from the background environment, photo-interpretation can substitute the costly field surveys, such as burned forest patches (Koutsias and Karteris, 1998; Koutsias, 2003). The prerequisites that need to be fulfilled to ensure validity of the results are (Koutsias and Karteris, 1998): (i) the sampling areas should be accurately determined on the satel-

lite image; (ii) the sampling size of all features should be about the same to avoid bias using certain algorithms; (iii) a satisfactory absolute sampling size should be obtained; and (iv) the sampling areas should represent the variability of all the features mapped on the satellite image. Based on the above, the training and validation datasets for the identification of irrigated fields can be sampled directly on the satellite images, based on the spectral characteristics of vegetation (described in the following sections).

2.3. Digital image enhancement

Apart from the original satellite image bands, several spectral enhancements have been tested as input to the mapping methods, aimed at improving the identification of irrigated land. Several other enhancement techniques have been proposed in literature (Richards, 1995; Jensen, 2005). However, the selected ones are among those well established in irrigation inventories, and can be operated using standard low cost digital image processing software, even shareware software.

2.3.1. Spectral indices

The Normalised Difference Vegetation Index (NDVI) is the most widely used vegetation index, and has already been mentioned in numerous studies related to monitoring the natural and cultivated vegetation (Silleos et al., 2006). It has been utilised extensively in irrigated system inventories

(Bastiaanssen, 1998) due to its advantages (strong correlation with vegetation parameters, simplicity in calculation and interpretation, and minimisation of topographic effects), although certain drawbacks have been reported, such as scaling problems, high sensitivity to background, and saturation over high biomass conditions (Huete et al., 2002). This vegetation index is based on the spectral properties of chlorophyll in the red and near-infrared wavelengths to highlight the abundant green photosynthesising vegetation, which in this case was the irrigated vegetation. It was calculated using the following equation:

$$\text{NDVI} = \frac{\text{NIR} - \text{RED}}{\text{NIR} + \text{RED}} \quad (1)$$

where NIR is the reflectance in near-infrared and RED is the reflectance in red wavelengths. The required bands are present in all the satellite images used in this work.

The Normalised Difference Wetness Index (NDWI) has also been suggested in similar studies, as it is sensitive to vegetation moisture content (Gao, 1996). This spectral index is based on the increased absorption of shortwave-infrared from leaf moisture (Hoffer, 1978). It uses the reflectance in the near- and shortwave-infrared bands of the image (Eq. (2)) to enhance the visualisation of vegetation with high moisture content, which in this case comprises the irrigated vegetation. Nageswara Rao and Mohankumar (1994) concluded that NDWI is superior to NDVI to identify irrigated land in India, despite its problem of assigning surface water with equal values to irrigated land.

$$\text{NDWI} = \frac{\text{NIR} - \text{SWIR}}{\text{NIR} + \text{SWIR}} \quad (2)$$

where NIR is the reflectance in near-infrared and SWIR is the reflectance in the shortwave-infrared wavelengths. The required bands are only present in the ASTER and Landsat images, as SPOT-4 does not record reflectance in the shortwave-infrared.

2.3.2. Principal component analysis

Principal component analysis (PCA) is a mathematical transformation of image data that has been applied in irrigated land inventories (Visser, 1989; Lourens, 1990). It has been primarily used for compressing the information of multispectral images into the first three principal components (PC1, PC2 and PC3). Using this transformation, most of the information can be simultaneously displayed using the screen's colour model (R, G, B = PC1, PC2, PC3). In this case, it has been used to improve the identification of irrigated land, under the assumption that since it is one of the major features of the image's spatial variability, it would be portrayed in one of the first three principal components. Comparing the principal components with the sampling areas, the one that displays the irrigated land with higher contrast to non-irrigated was selected.

2.4. Identification of irrigated area

Among the large collection of methods for automated land features mapping (information extraction) proposed (Richards, 1995; Jensen, 2005), those well established in irri-

gation inventories and easily operated with standard low cost digital image processing software, even shareware software, have been incorporated in the methodology.

2.4.1. Supervised classification

Supervised spectral classification was used to automatically group pixels of multispectral images into groups of pre-defined classes, based on the variation of reflectance among the spectral bands. Spectral signatures for land cover classes of interest were described with the use of training sampling areas, which were: irrigated crops, non-irrigated crops, natural vegetation, bare land, settlements or infrastructure, and water. It is noted that more classes than those of interest (irrigated and non-irrigated crops) were defined to keep the within-class variability low, and thus minimise errors of misclassification. Next, the pixels of each input image were assigned to classes using a probabilistic maximum likelihood algorithm. Finally, the individual classes that formed the "non-irrigated" class were grouped together to produce the map of irrigated and non-irrigated areas.

2.4.2. Unsupervised classification

Unsupervised classification was also used to automatically group pixels of multispectral images into clusters of similar reflectance, through the use of standard statistical approaches, without relying on pre-defined classes. The ISO-DATA (Iterative Self-Organising Data Analysis Technique) (Tou and Gonzalez, 1974), clustering method was utilised, which uses spectral distances in an iterative process of assigning the pixels into classes, until spectral distance patterns on the image gradually emerge. It is noted that more classes than those of interest were requested by the classifier to achieve a detailed identification of spectral variation. Finally, the spectral classes were assigned to land cover classes using photo-interpretation of the training sampling areas, and after grouping into the classes of interest, the map of irrigated and non-irrigated areas was produced.

2.4.3. Thresholding

Information extraction using thresholding is applied to single-layered images, usually after their enhancement. It is based on selecting a threshold value on the histogram of the input image, and then using this value for slicing the histogram into two parts, each assigned to a class of interest. The respective pixels belonging to either side of the threshold value on the histogram are assigned to one of the two classes, formulating the resulting thematic map.

The selection of the threshold value was performed separately for each input image. Using the training sampling areas, the data values on the input image were displayed in a single graph as two histograms, one for irrigated and one for non-irrigated area. It is noted that the non-irrigated area comprised several land cover classes (non-irrigated winter crops, natural vegetation, bare land, settlements or infrastructure, and water). The threshold value that was selected was the point of equal probability to belong in each histogram based on their distribution, which was often in the area between the two histograms, or the median between their main volumes. Visual inspection of the irrigated area map, mainly on the fringe of irrigated land and the agricultural road network,

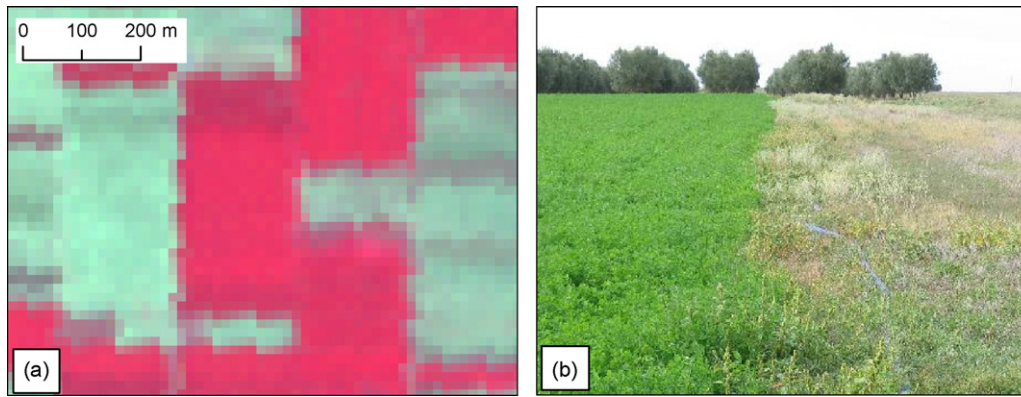


Fig. 3 – View of irrigated vs. non-irrigated fields on a satellite image (standard false colour composite) (a) and on the field (b).

indicated minor changes of the threshold value, which helped to improve the final result.

2.4.4. Accuracy assessment

Methods for automated land features mapping are concluded with an accuracy assessment of their result (Congalton, 1991). The validation sampling points were used on this account. For each validation point, the class that was indicated on the irrigated area map was compared with the class that had been assigned on the point by the photo-interpreter. The comparison was facilitated with an error matrix, which compares on a tabular form the relationship between reference data (validation dataset) and the corresponding results from an automated mapping method (irrigated area map) (Richards, 1995). From the error matrix, the overall accuracy of the map and the kappa hat statistic (\hat{k}) were calculated. The overall accuracy is defined as the percentage of validation points that are correctly classified and describes the accuracy of the contents of the map, while the \hat{k} statistic represents the probability that the classification accuracy is due to chance, and reflects the reliability of the map. It can be calculated from the following equation:

$$\hat{k} = \frac{N \sum_{i=1}^r x_{ii} - \sum_{i=1}^r x_{i+} \cdot x_{+i}}{N^2 - \sum_{i=1}^r (x_{i+} \cdot x_{+i})} \quad (3)$$

where r is the number of rows in the error matrix, x_{ii} is the number of observations in row i and column i , x_{i+} and x_{+i} are the marginal totals of row i and column i , respectively, and N is the total number of observations (Cohen, 1960; Congalton, 1991).

3. Results and discussion

3.1. Formulation of the methodology for mapping irrigated area in the test site

The basic assumption for mapping irrigated areas using visible and infrared satellite images in a Mediterranean basin with a semiarid summer, is that the irrigated land would hold the only concentration of green photosynthesising vegetation in the agricultural area. Indeed, as irrigated crops reach full

growth in late summer (taking advantage of high incoming solar radiation) that is almost arid, and farmers take every effort to use the scarce water resources efficiently, there is a vivid contrast to the dried-up background (Fig. 3). Therefore, the irrigated area is identified from non-irrigated based on the spectral behaviour of the result of irrigating the land, which is the green vegetation.

The training sampling areas were identified in 50 key locations on the ASTER image, to cover the spectral variability of irrigated fields, as well as the other land cover types of the agricultural area of the test site. Thus, the training sample size consisted of 3320 pixels for irrigated and 3639 for non-irrigated. An independent dataset was used for validation of the results. This was identified on the image using random sampling, to eliminate the analyst's preference to the centre of homogeneous areas, thus avoiding the difficult fringes. Based on the previous assumption and using careful photo-interpretation of the satellite image, each point in the validation dataset was assigned to either irrigated or non-irrigated class. In total, 250 validation points were identified on the ASTER image.

3.1.1. Comparison of methods

Since the information layers (image bands and their enhancements) and mapping methods described here have been reported as advantageous in irrigated land inventories, all possible combinations of automated land features mapping methods were applied on the original and spectrally enhanced images in order to identify the optimum. Not all combinations were possible, due to the design of spectral classification methods to be applied on multispectral images, and the design of thresholding to be applied on single-layer images. Each combination that was tested has produced an irrigated area map, and its accuracy was assessed using the validation dataset. The irrigated area, overall accuracy, and \hat{k} statistic are displayed in Table 1 for the possible combinations. Supervised and unsupervised classification of the PCA image was performed using the first three principal components (first three bands), while thresholding was performed on the second principal component (second band), which was identified visually as the one that displays the highest contrast of irrigated area to the background.

Table 1 – Irrigated area acreage (km²), overall accuracy (%), and the \hat{k} statistic (no units) for every combination of mapping methods on the information layers

Information layers	Mapping methods		
	Supervised classification	@Unsupervised classification	Thresholding ^a
Image bands	83.40 km ² 93.6% $\hat{k} = 0.872$	94.08 km ² 90.1% $\hat{k} = 0.801$	–
NDVI	–	–	78.28 km ² 96.4% $\hat{k} = 0.928$
NDWI	–	–	83.08 km ² 94.4% $\hat{k} = 0.887$
CA ^a	79.80 km ² 95.2% $\hat{k} = 0.904$	82.60 km ² 94.8% $\hat{k} = 0.896$	74.14 km ² 98.4% $\hat{k} = 0.967$

A dash indicates an impossible combination.

^a Thresholding on PCA was performed on PC2.

The differences among the irrigated area estimates are generally low (standard deviation of 6.19 km²), indicating that all combinations of mapping methods on information layers have produced very good results, exceeding 90% accuracy (Table 1). The resulting maps are also very reliable, since all \hat{k} values are high. Thresholding the PC2 has provided the highest accuracy, reaching 98.4% (Fig. 4). Several other combinations have reached 95% accuracy, mostly using thresholding, or the PCA, which is an indication that these could be the optimum techniques for mapping the irrigated area in the test site. Unsupervised classification has produced the lowest accuracies and had a tendency to overestimate the irrigated area, probably due to the mixture of spectral classes of interest within the clusters provided by the algorithm. Thresholding the NDWI has also resulted in an overestimation of the irrigated area, probably due to the lower spatial resolution of shortwave-infrared band (30 m as opposed to 15 m for the others). The general trend was for most combinations to overestimate the irrigated area, possibly due to mixed pixels, or weeds growing around the fringe of irrigated fields, taking advantage of the low spatial precision in irrigation appli-

cations. This was confirmed with visual assessment of the irrigated area maps.

3.1.2. Improvement and visualisation of results

Although a single image has been sufficient for mapping irrigated areas in south India when it is acquired in the period of crop maturity (Thiruvengadachari, 1981), it has been noted that a second image of the same cropping season is essential to detect irrigated crops of variable cropping calendars (Martinez-Casasnovas et al., 2005). Alfalfa is a common crop in the test site, which has a monthly harvesting cycle. Thus, there is a possibility that several alfalfa fields would not be detected if the image were acquired immediately after one of their harvests. Therefore, a second image of the same cropping season (SPOT, acquired on September 23, 2003) was incorporated to minimise this possibility. Since both satellite images have similar spatial and spectral characteristics, the optimum combination of mapping method on image enhancement was applied, based on the previous results. Using a subset of the training and validation datasets that covered the spatial extents of the SPOT image, the irrigated

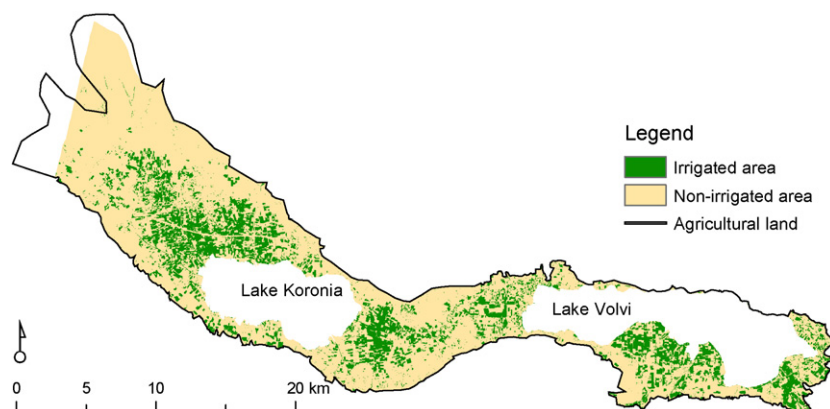


Fig. 4 – Irrigated area map in Mygdonia basin using thresholding of PC2 of the ASTER image.

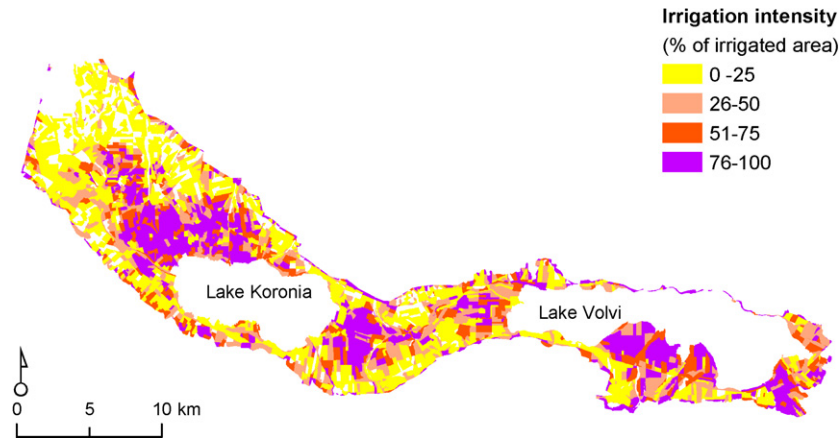


Fig. 5 – Irrigation intensity map in Mygdonia basin for 2003.

map for September was produced (overall accuracy of 97.9%, $\hat{k} = 0.957$).

Using overlay geographic analysis, the irrigated area maps of July (ASTER) and September (SPOT) were compared, based on their area of overlap (58% of agricultural land). An additional irrigated area of 4.46 km² (13.4% of the equivalent irrigated area for July) was identified from the September image, revealing that a significant portion of irrigated area would not have been depicted using a single satellite image.

Finally, the irrigated area map was displayed as irrigation intensity, which improves the visualisation of the pressure acting on the natural resources of the basin. Irrigation intensity was defined as the percentage of agricultural land that is being irrigated, and was estimated using the agricultural blocks as spatial units. These are continuous portions of homogeneous land use, delimited by geographic irregularities, roads, or other elements of discontinuity. They have been identified on 1:5,000 scale photomaps (Masson, 2002) and their mean area is 0.12 km² in the test site. In the area around Lake Volvi that was not covered by the SPOT image, an additional 13.4% of irrigated land was added, making the assumption

that the agricultural pattern is uniform in the basin. The overall estimate of irrigated land for Mygdonia site is 84.07 km².

The highest intensities in Mygdonia basin were observed around the streams feeding the lakes (Fig. 5), where groundwater levels are shallower, and thus abstractions require less energy. However, these were resulting in the highest environmental impact to the wetland-lakes ecosystem, as they contributed to the depletion of the main aquifers that feed Lake Koronia (Zalidis et al., 2004; Alexandridis et al., 2007).

3.2. Operation of methodology at the demonstration site

Thresholding the second PC of the Landsat images was used to produce the irrigated area map of the Strimonas site. The threshold was selected using 50 training areas identified on the images, and the accuracy of the result was assessed using 250 validation points. An additional irrigated area of 62.27 km² (9.5% of the common area of overlap) was identified on the June map, which was missed in the August map. This is mainly due to freshly harvested alfalfa, and to a lesser extent to early maize. Overlay analysis of the individual maps of June and

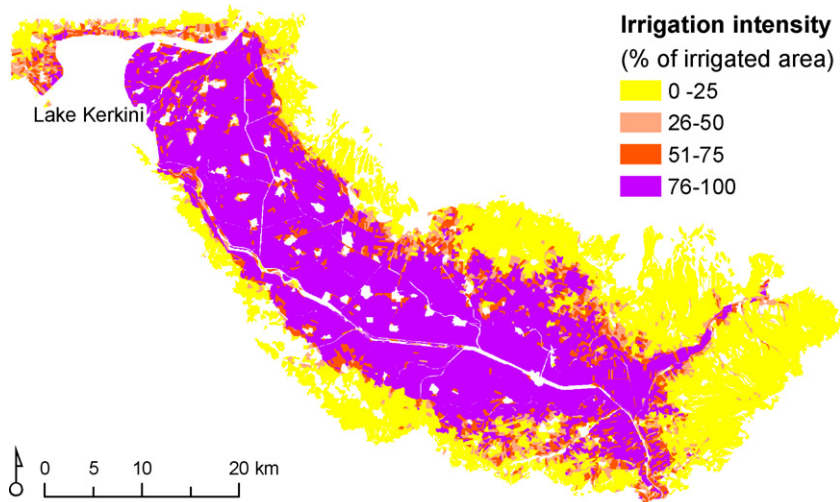


Fig. 6 – Irrigation intensity map in Strimonas basin for 2000.

August has provided the irrigated area map for year 2000, revealing a total of 833.46 km² with an overall accuracy of 97.1% ($\hat{k} = 0.942$). Combining the irrigated area map with the agricultural lots of the site, the irrigation intensity map was created (Fig. 6). The lowest values of irrigation intensity (less than 50%) appear at the upper zones of the basin, where the collective irrigation networks do not reach and irrigation water is pumped from private wells. In these areas water costs are higher than those supplied by a collective irrigation network, thus providing a counterincentive for irrigating. The highest intensities (more than 90%) appear in areas where rice or cotton is cultivated. Indeed, rice paddies are grouped in contiguous large plots because secondary salinisation in adjacent fields prevents the installation of any other crop but rice. A reason for very high intensities in the non-rice regions is the water fees charging system. Farms owned within the canal command of collective irrigation systems are charged by the irrigable area, even if they do not wish to use any water, which promotes the intensification of agriculture.

The high water demands of areas irrigated from artificial lake Kerkini puts pressure on water managers to keep the lake's level extremely high in spring, thus flooding the riparian forest of the lake's wetland for long periods. As a result of the prolonged inundation, this important habitat for wildlife has decreased in size in the last decades (Keramitsoglou et al., 2006). Another environmental implication in areas of high irrigation intensity is the discharge of drained water, decreasing the quality of surface and groundwater systems.

3.3. Evaluation of methodology and limitations

The basic assumption, that irrigated land can be identified by the result of irrigation, i.e. the existence of green photosynthesising vegetation in the semiarid summer, has been confirmed in previous work (Heller and Johnson, 1979; Lourens, 1990). In these studies it has been justified that since most irrigated land occurs in arid to semiarid areas of the world, the contrast between irrigated cropland and surrounding dry land is high. However, there are potential limitations. The vicinity of agricultural land to a wetland could be a source of confusion, as the shallow groundwater level and numerous streams may support green natural vegetation through the semiarid summer. Indeed, in the Mygdonia site, wetland vegetation had already been identified and excluded from the analyses using photo-interpretation (Alexandridis et al., 2007), as it could not have been discerned from irrigated vegetation. On the other hand, it was assumed that irrigated vegetation would be green and photosynthesising enough to provide a strong infrared reflection. Even during attacks from pests or insects, or on low fertility soils, farmers would take every precaution to guarantee a high yield, thus verifying the assumption. For the same reasons, a farmer growing summer crops in an area with developed water resources, would fully irrigate (Selby, 1949).

The methodology is also based on the identification of training and validation datasets directly on the satellite image using photo-interpretation. This technique has already been used successfully in mapping burned forest (Koutsias and Karteris, 1998; Koutsias, 2003). However, to prove its reliability in mapping irrigated area, the technique was validated using

reference data acquired during field surveys. The validation process used a subset (149 points in Mygdonia site surveyed on August 2003) of a regular survey that identifies land cover on a national level using systematic sampling for the Integrated Administration and Control System, supervised in Greece by the Ministry of Agriculture (Tsiligirides, 1998). The surveyed locations were assigned to a class of interest (irrigated or non-irrigated) with photo-interpretation of the ASTER image. Comparison of the photo-interpretation class with the field surveyed class revealed a match of 98.6% ($\hat{k} = 0.973$), which supports the validity of the method.

The number of images required per irrigation season is a subject that affects the results and the cost of the project. In this work, crops that deviate from the usual cropping calendar (early maize) or that may be harvested regularly (alfalfa) have necessitated the use of a second image in the same irrigation season. Similar problems have been reported with sunflower crops in Spain (Martinez-Casasnovas et al., 2005) and double cropped land in India (Thiruvengadachari, 1981; Nageswara Rao and Mohankumar, 1994). However, it remains to be investigated whether a third image in the irrigation season would contribute to the improvement of the results. The variable atmospheric conditions among the dates of acquisition did not necessitate atmospheric or radiometric correction, as the images were processed independently (Song et al., 2001).

Costs associated with this work were on the lower side of the already reported as low-cost remote sensing mapping applications (Mumby et al., 1999; Wright et al., 2003). This was due to that fact that no field surveys were necessary, and to the selection of low cost satellite imagery (to cover Mygdonia site, ASTER and SPOT cost was 0.65 and 1.81 € per km² of agricultural area, respectively, and to cover Strimonas site, Landsat scene cost was 0.75 € per km² of agricultural area). In addition, the digital image processing techniques selected had low requirements in software (for instance, Idrisi Andes = 850 €, GRASS is shareware) and specialised personnel (total of 3 person-weeks for development and 1 person-week for application).

The methodology can be applied to other basins of the Mediterranean, where the assumptions hold true. In addition, it can be applied to previous years when using archived satellite images, even when field surveys had not been conducted. It has been proven successful in larger scale basins (Strimonas), using lower spatial resolution satellite images. However, more sophisticated methodologies may be required for monitoring irrigated area of large basins expanding in several agro-climatic zones, due to difficulties that arise, such as scattered cloud cover and inconsistent crop cycles (Droogers, 2002; Thenkabail et al., 2005).

4. Conclusions

A methodology was developed to cover the needs for irrigated area monitoring of the recent EU directives and policies. The desired features of the methodology were: to be objectively repeatable with low cost data and methods, providing high accuracy results. The methodology was formulated under the assumption that irrigated land can be identified by the result of irrigation, i.e. the existence of green photosynthesising veg-

etation in the semiarid summer, thus avoiding costly field surveys, and using low cost satellite imagery.

The proposed methodology was successful in estimating the irrigated area in two basins in the Mediterranean with conflicting agronomic and ecological interests. The methodology was performed in two basins of different scales, using various satellite images as input, and achieving results of high accuracy (up to 98.4%) and reliability (\hat{k} up to 0.967). However, a single image acquired at full growth of the irrigated crops may not be sufficient to map the total of the irrigated area, mainly due to crops of uncommon cropping calendar. In both sites, a second image in the irrigated season has revealed an additional irrigated area, as much as 13.4%.

The implementation of the developed methodology and consequently the regular update of irrigated area maps in Mediterranean basins provides information essential to understanding the complex issues between agriculture and the environment. Moreover, it constitutes the basis of an efficient tool in management and protection of the scarce water resources, and can provide guidance for setting priorities in water policy and influence land use planning.

Acknowledgements

The authors express their gratitude to S. Veopoulou, E. Zogia, S. Kalimanis, and M. Christoforou for their contribution in digital image processing. The ASTER satellite image was distributed by the Land Processes Distributed Active Archive Center (LP DAAC), located at the U.S. Geological Survey's EROS Data Center. The Landsat images were distributed by Global Land Cover Facility (GLCF). The Greek Ministry of Agriculture is acknowledged for providing available ground survey data and a subset of the SPOT image. Authors are also thankful to the anonymous reviewers for their constructive comments on the original manuscript.

REFERENCES

- Alexandridis, T.K., Takavakoglou, V., Crisman, T.L., Zalidis, G.C., 2007. Remote sensing and GIS techniques for selecting a sustainable scenario for Lake Koronia, Greece. *Environmental Management* 39, 278–290.
- Babajimopoulos, C., Budina, A., Kalfountzos, D., 1995. SWBACROS: a model for the estimation of the water balance of a cropped soil. *Environmental Software* 10, 211–220.
- Bastiaanssen, W.G.M., 1998. Remote Sensing in Water Resources Management. The state of the art International Water Management Institute, Colombo, Sri-Lanka, 118 p.
- Bastiaanssen, W.G.M., 1999. The use of remote sensing to improve irrigation water management in developing countries. In: Nieuwenhuis, G.A., Vaughan, R.A., Molenaar, M. (Eds.), *Operational Remote Sensing for Sustainable Development*. Balkema, Rotterdam, pp. 3–17.
- Bastiaanssen, W.G.M., Molden, D.J., Makin, I.W., 2000. Remote sensing for irrigated agriculture: examples from research and possible applications. *Agricultural Water Management* 46, 137–155.
- Biggs, T.W., Thenkabail, P.S., Gumma, M.K., Scott, C.A., Parthasaradhi, G.R., Turral, H.N., 2006. Irrigated area mapping in heterogeneous landscapes with MODIS time series, ground truth and census data, Krishna Basin, India. *International Journal of Remote Sensing* 27, 4245–4266.
- Cohen, J., 1960. A coefficient of agreement for nominal scales. *Educational and Psychological Measurement* 20, 37–46.
- Congalton, R.G., 1991. A review of assessing the accuracy of classifications of remotely sensed data. *Remote Sensing of Environment* 37, 35–46.
- Droogers, P., 2002. Global irrigated area mapping: overview and recommendations, Working Paper 36 International Water Management Institute, Colombo, Sri Lanka. URL: <http://www.iwmi.cgiar.org/pubs/working/WOR36.pdf>.
- Droogers, P., Bastiaanssen, W.G.M., Beyazgul, M., Kayam, Y., Kite, G.W., Murray-Rust, H., 2000. Distributed agro-hydrological modeling of an irrigation system in western Turkey. *Agricultural Water Management* 43, 183–202.
- EC, 1999a. European Council Regulation (EC) No 1251/1999 of 17 May 1999 establishing a support system for producers of certain arable crops. *Official Journal L* 160, 26/06/1999, p.1–14.
- EC, 1999b. European Council Regulation (EC) No 1257/1999 of 17 May 1999 on support for rural development from the European Agricultural Guidance and Guarantee Fund (EAGGF) and amending and repealing certain Regulations. *Official Journal L* 160, 26/06/1999 p.80–101.
- EC, 2000. Directive 2000/60/EC of the European Parliament and of the Council of 23 October 2000 establishing a framework for Community action in the field of water policy. *Official Journal L* 327, 22/12/2000 p.0001–0073.
- EC, 2003. European Council Regulation 1782/03: Reform of the CAP, which introduces a single payment scheme, cross compliance and Farm Advisory System. *Official Journal L* 270, 21/10/03, p.1.
- EEC, 1979. Council Directive 79/409/EEC of 2 April 1979 on the conservation of wild birds. *Official Journal L* 103, 25/04/1979 p.0001–0025.
- EEC, 1992. Council Directive 92/43/EEC of 21 May 1992 on the conservation of natural habitats and of wild fauna and flora. *Official Journal L* 206, 22/07/1992 p.0007–0050.
- El-Magd, I.A., Tanton, T.W., 2003. Improvements in land use mapping for irrigated agriculture from satellite sensor data using a multi-stage maximum likelihood classification. *International Journal of Remote Sensing* 24, 4197–4206.
- FAO, IFAD, 2006. Water for food, agriculture and rural livelihoods. In: *The United Nations world water development report 2: water, a shared responsibility*. UNESCO and Berghahn Books. URL: <http://unesdoc.unesco.org/images/0014/001454/145405E.pdf>.
- Gao, B.C., 1996. NDWI—a normalized difference water index for remote sensing of vegetation liquid water from space. *Remote Sensing of Environment* 58, 257–266.
- Heller, R.C., Johnson, K.A., 1979. Estimating irrigated land acreage from Landsat imagery. *Photogrammetric Engineering and Remote Sensing* 45, 1379–1386.
- Hoffer, R.M., 1978. Biological and physical considerations in applying computer-aided analysis techniques to remote sensor data. In: Davis, S.M., Swain, P.H. (Eds.), *Remote Sensing: the Quantitative Approach*. McGraw-Hill International Book Co, London; New York, pp. 227–289.
- Huete, A., Didan, K., Miura, T., Rodriguez, E.P., Gao, X., Ferreira, L.G., 2002. Overview of the radiometric and biophysical performance of the MODIS vegetation indices. *Remote Sensing of Environment* 83, 195–213.
- Jensen, J.R., 2005. *Introductory Digital Image Processing: a Remote Sensing Perspective*, third ed. Prentice-Hall, Inc., New Jersey, 544 p.
- Keramitsoglou, I., Sarimveis, H., Kiranoudis, C.T., Kontoes, C., Sifakis, N., Fitoka, E., 2006. The performance of pixel window algorithms in the classification of habitats using VHRS imagery. *ISPRS Journal of Photogrammetry and Remote Sensing* 60, 225–238.

- Kite, G., 2000. Using a basin-scale hydrological model to estimate crop transpiration and soil evaporation. *Journal of Hydrology* 229, 59–69.
- Koutsias, N., 2003. An autologistic regression model for increasing the accuracy of burned surface mapping using Landsat Thematic Mapper data. *International Journal of Remote Sensing* 24, 2199–2204.
- Koutsias, N., Karteris, M., 1998. Logistic regression modelling of multitemporal Thematic Mapper data for burned area mapping. *International Journal of Remote Sensing* 19, 3499–3515.
- Lianos, T.P., Parliarou, D., 1986. Farm size structure in Greek agriculture. *European Review of Agricultural Economics* 13, 233–248.
- Lourens, U., 1990. Using Landsat TM to monitor irrigated land at the individual farm level. In: Menenti, M. (Ed.), *Remote Sensing in Evaluation and Management of Irrigation*. Instituto Nacional del Ciencia y Tecnicas Hidricas, Mendoza, Argentina, pp. 231–235.
- Martinez-Casasnovas, J.A., Martin-Montero, A., Casterad, M.A., 2005. Mapping multi-year cropping patterns in small irrigation districts from time-series analysis of Landsat TM images. *European Journal of Agronomy* 23, 159–169.
- Masson, J., 2002. Report of the JRC activities on Olive GIS in the 5 Member States (FR, GR, I, SP, PO). Annual report v1.2, pp. 38. Institute for the Protection and the Security of the Citizen, Joint Research Centre, Ispra, Italy. URL: http://agrifish.jrc.it/Documents/Olivine/OLISIG_rapport_Act.2002_2v.pdf.
- Mitrakis, N.E., Topaloglou, C.E., Alexandridis, T.K., Theocharis, J.B., Zalidis, G.C., 2008. Decision fusion of GA self-organizing neuro-fuzzy multilayered classifiers for land cover classification using textural and spectral features. *IEEE Transactions on Geoscience and Remote Sensing* 46, 2137–2152.
- Mumby, P.J., Green, E.P., Edwards, A.J., Clark, C.D., 1999. The cost-effectiveness of remote sensing for tropical coastal resources assessment and management. *Journal of Environmental Management* 55, 157–166.
- Nageswara Rao, P.P., Rao, V.R., 1987. Rice crop identification and acreage estimation using remotely-sensed data from Indian cropping patterns. *International Journal of Remote Sensing* 8, 365–370.
- Nageswara Rao, P.P., Mohankumar, A., 1994. Cropland inventory in the command area of Krishnarajasagar project using satellite data. *International Journal of Remote Sensing* 15, 1295–1305.
- Richards, J.A., 1995. *Remote Sensing Digital Image Analysis: an Introduction*, second ed. Springer-Verlag, Berlin; London, 340 p.
- Seckler, D., Barker, R., Amarasinghe, U., 1999. Water scarcity in the twenty-first century. *International Journal of Water Resources Development* 15, 29–42.
- Selby, H.E., 1949. The importance of irrigation in the economy of the west. *Journal of Farm Economics* 31, 955–964.
- Shiklomanov, I.A., 2000. Appraisal and assessment of world water resources. *Water International* 25, 11–32.
- Silleos, N.G., Alexandridis, T.K., Gitas, I.Z., Perakis, K., 2006. Vegetation indices: advances made in biomass estimation and vegetation monitoring in the last 30 years. *Geocarto International* 21, 21–28.
- Song, C., Woodcock, C.E., Seto, K.C., Lenney, M.P., Macomber, S.A., 2001. Classification and change detection using Landsat TM data: when and how to correct atmospheric effects? *Remote Sensing of Environment* 75, 230–244.
- Thenkabail, P.S., Schull, M., Tural, H., 2005. Ganges and Indus river basin land use/land cover (LULC) and irrigated area mapping using continuous streams of MODIS data. *Remote Sensing of Environment* 95, 317–341.
- Thiruvengadachari, S., 1981. Satellite sensing of irrigation patterns in semiarid areas: an Indian study. *Photogrammetric Engineering and Remote Sensing* 47, 1493–1499.
- Tou, J., Gonzalez, R., 1974. *Pattern Recognition Principles*. Addison-Wesley Publishing Company, Reading, Massachusetts, 377 p.
- Tsiligirides, T.A., 1998. Remote sensing as a tool for agricultural statistics: a case study of area frame sampling methodology in Hellas. *Computers and Electronics in Agriculture* 20, 45–77.
- Vidal, A., Perrier, A., 1990. Irrigation monitoring by following the water balance from NOAA-AVHRR thermal infrared data. *IEEE Transactions on Geoscience and Remote Sensing* 28, 949–954.
- Visser, T.N.M., 1989. *Appraisal of the Implementation of Water Allocation Policies*. ICW (Instituute voor Cultuurtechniek en Waterhuishouding), Wageningen, The Netherlands, 54 p.
- Wright, G.G., Matthews, K.B., Cadell, W.M., Milne, R., 2003. Reducing the cost of multi-spectral remote sensing: combining near-infrared video imagery with colour aerial photography. *Computers and Electronics in Agriculture* 38, 175–198.
- Xiao, X., Boles, S., Froking, S., Salas, W., Moore, B., Li, C., He, L., Zhao, R., 2002. Observation of flooding and rice transplanting of paddy rice fields at the site to landscape scales in China using VEGETATION sensor data. *International Journal of Remote Sensing* 23, 3009–3022.
- Zalidis, G.C., Takavakoglou, V., Alexandridis, T.K., 2004. Revised Restoration Plan of Lake Koronia. Final report submitted to the Prefecture of Thessaloniki, Thessaloniki, Greece (In Greek, English Summary).